Characteristics of the 1997/1998 El Niño cloud distributions from SAGE II observations

Pi-Huan Wang,[1] Patrick Minnis,[2] Bruce A. Wielicki,[2] Takmeng Wong,[2] Robert D. Cess,[3] Minghua Zhang,[3] Lelia B. Vann,[2] and Geoffrey S. Kent[1]

Received 5 January 2002; revised 22 July 2002; accepted 4 August 2002; published 8 January 2003.

[1] The present study examines the characteristics of cloud distributions with emphasis on cloud longwave radiative forcing (CLRF) during the peak of the 1997/1998 El Niño in relation to climatological conditions, based on measurements from the Stratospheric Aerosol and Gas Experiment (SAGE) II. The observed distinct cloud occurrence and CLRF during this unusual 1997/1998 El Niño constitutes a unique data set for validating and improving cloud-radiation-climate interactions in general circulation and climate models. Using the solar occultation technique, the SAGE II satellite instrument is capable of providing measurements with a 1-km vertical resolution facilitating the analysis with sufficient vertical as well as near global scale (70°S–70°N) details. The present study indicates (1) above normal high-altitude opaque cloud occurrence over the eastern tropical Pacific and an opposite situation over the Pacific warm pool, leading to a distribution of the cumulative opaque cloud anomalies above 3 km generally consistent with the pattern of observed tropical sea surface temperature and precipitation anomalies; (2) a similar behavior in the subvisual cloud distributions near the tropical tropopause; (3) a zonally averaged cloud distribution that is characterized by reduced opaque clouds at low latitudes, except in the southern tropics below 10 km, and by enhanced opaque clouds at high latitudes, along with increased subvisual clouds in the southern tropics and decreased subvisual clouds in the northern subtropics in the upper troposphere; and (4) a geographic distribution of model-calculated CLRF anomalies that resembles closely that inferred from the Earth Radiation Budget Experiment and the Clouds and the Earth's Radiant Energy System. A discussion on the influence of the El Niño on large-scale mean tropospheric circulations is also provided. *INDEX TERMS:* 0320 Atmospheric Composition and Structure: Cloud physics and chemistry; 1630 Global Change: Impact phenomena; 3309 Meteorology and Atmospheric Dynamics: Climatology (1620); 3319 Meteorology and Atmospheric Dynamics: General circulation; 3359 Meteorology and Atmospheric Dynamics: Radiative processes; *KEYWORDS:* El Niño, clouds, climate, remote sensing

Citation: Wang, P.-H., P. Minnis, B. A. Wielicki, T. Wong, R. D. Cess, M. Zhang, L. B. Vann, and G. S. Kent, Characteristics of the 1997/1998 El Niño cloud distributions from SAGE II observations, *J. Geophys. Res.*, *108*(D1), 4009, doi:10.1029/2002JD002501, 2003.

1. Introduction

[2] El Niños are known for leading to severe weather anomalies on a global scale [e.g., *Peng and Van den Dool*, 1998]. The 1997/1998 El Niño was perhaps the most intense one on record [*Kousky*, 1998; *Bell et al.*, 1999]. Its scale and strength caught the scientific community by surprise. Studies based on sea surface temperatures (SST) suggest that the period March–May 1997 can be regarded as the onset phase of the 1997/1998 El Niño, with a mature phase between June 1997 and April 1998 and a decay phase during May–June 1998 [e.g., *Kousky*, 1998]. Although forecast models had some success in predicting an El Niño for 1997/1998, the predicted event was much weaker and later than was actually observed [*McPhaden*, 1998]. The El Niño was so intense that it produced a mean tropical clear-sky outgoing longwave radiation (OLR) enhancement of 2 W/m^2 in early 1998 [*Wong et al.*, 2000], and an even larger all-sky increase of 6 to 8 W/m^2 in early 1998 [*Wang et al.*, 2002; *Wielicki et al.*, 2002]. This increase in OLR is accompanied by an increase of about 1°C in the mean tropical tropospheric temperature, the largest mean temperature enhancement of three El Niños in the 1980s and 1990s [*Wang et al.*, 2002].

[3] A recent study, using upwelling shortwave and longwave radiation measurements over the Pacific warm pool from the satellite instruments of the Earth Radiation Budget Experiment (ERBE) and the Clouds and the Earth's Radiant

[1]Science and Technology Corporation, Hampton, Virginia, USA.
[2]Atmospheric Sciences Competency, NASA Langley Research Center, Hampton, Virginia, USA.
[3]Marine Sciences Research Center, State University of New York, Stony Brook, Stony Brook, New York, USA.

0148-0227/03/2002JD002501$09.00

Energy System (CERES) suggests a drastically perturbed cloud vertical distribution, with much reduced high-altitude clouds, during the 1997/98 El Niño [*Cess et al.*, 2001a]. Such a perturbed cloud vertical structure was most recently confirmed by cloud distributions derived from the Stratospheric Aerosol and Gas Experiment (SAGE) II data [*Cess et al.*, 2001b]. In addition, an opposite behavior of the cloud vertical structure over the Eastern Pacific was also revealed by the SAGE II cloud observations, consistent with a severely altered Walker circulation in the tropics [*Bell et al.*, 1999; *Cess et al.*, 2001b] during the 1997/1998 El Niño.

[4] Both SAGE II and ERBE are on board the Earth Radiation Budget Satellite (ERBS). While the ERBE instrument monitors the Earth radiation balance [*Barkstrom*, 1984], the SAGE II sensor measures the properties of aerosols and gaseous species, including O_3, H_2O, and NO_2, important for understanding and interpreting atmospheric radiative properties [*McCormick*, 1987]. Because of the microphysical relationship between aerosols and clouds, the SAGE II tropospheric observations also contain samples of cloud extinction coefficients at 0.525 and 1.02 μm [*Kent et al.*, 1993; *Wang et al.*, 1994, 1998a]. Furthermore, it is understood that the presence of optically thick clouds along the tangential viewing path of the SAGE II instrument terminates the solar occultation profile measurement [*McCormick et al.*, 1979]. Therefore, the SAGE II observations provide information on opaque cloud occurrence in addition to optically thin clouds [*Wang et al.*, 1995b].

[5] While opaque clouds, particularly those associated with deep convection, strongly influence the Earth radiation budget [e.g., *Cess et al.*, 2001b] and vertical distributions of tropospheric chemical species, [e.g., *Wang et al.*, 1995a], the persistent presence of optically thin clouds can also have more subtle effects on atmospheric processes. They could affect both ozone concentration through heterogeneous chemical reactions in the tropopause region [*Solomon et al.*, 1997; *Bregman et al.*, 2002] and the water vapor budget in the lower stratosphere [*SPARC*, 2000], and can have a minor impact on the Earth radiation budget [*Wang et al.*, 1996]. Furthermore, previous studies indicate that the SAGE II 1.02-μm tropospheric measurement statistics reveal general geographic variations of cloud occurrence with distinct features related to tropospheric circulations including the Hadley cell and the Walker circulation [*Wang*, 1994; *Wang et al.*, 1995b]. Based on the intimate relationship between opaque cloud occurrence and large-scale convective circulation, a method has been developed for diagnosis of tropospheric mean meridional circulation based on the zonal mean distribution of the SAGE II tropospheric measurement frequency [*Wang et al.*, 1998b].

[6] The objectives of the present study are (1) to explore the characteristics of cloud distributions, including both optically thin and opaque clouds, and the large-scale mean tropospheric circulations for the 1997/1998 El Niño period, using SAGE II observations; and (2) to quantitatively assess the connection between the cloud and outgoing longwave radiation anomalies during the 1997/1998 El Niño to improve the understanding of the cloud-radiation interactions. The analyses of the SAGE II cloud observations and the large-scale circulation for the 1997/98 El Niño are presented in section 2, followed by an investigation of the cloud-radiation interactions in terms of cloud longwave radiative forcing (CLRF) for the El Niño in section 3. The conclusions of the present study and remarks are provided in section 4.

2. Cloud Data and Analysis

[7] The SAGE II 0.525- and 1.02-μm data have been analyzed to provide mean vertical profiles of cloud occurrence at a seasonal time scale [*Kent et al.*, 1993; *Wang et al.*, 2001]. The SAGE II observations contain two general groups of clouds, namely, opaque clouds (OC) and subvisual clouds (SVC). They are separated at a vertical optical depth of about 0.025 at 1.02-μm wavelength. According to the cirrus cloud classification of *Sassen and Cho* [1992], the SAGE II opaque clouds generally include all types of clouds, except optically thin subvisual clouds [*Wang et al.*, 1996]. A two-wavelength method has been developed by *Kent et al.* [1993] for identifying subvisual cloud data from SAGE II measurements. *Wang et al.* [1995b] developed a method for inferring the vertical distribution of optically thick clouds based on SAGE II 1.02-μm observations. This method has been further reviewed in detail by *Wang et al.* [2001].

[8] The present analysis for the 1997/98 El Niño uses the cumulative opaque cloud (COC) occurrence above a given altitude, as in the study of *Cess et al.* [2001b]. In addition, variations in the occurrence of SVCs are also investigated. The COC is a ratio of the difference between the total number of SAGE II overpasses and the number of the sample events that reached a given altitude over a specified geographic area to the total number of overpasses over the same region [*Wang et al.*, 2001]. The difference between the total number of overpasses and the frequency of the sample events at a given altitude is essentially the number of SAGE II observations that were terminated by the presence of opaque clouds above the given altitude. Thus, the sum of the cumulative cloud probability and the SAGE II measurement probability at a given altitude is unity [*Wang et al.*, 2001]. In the case of SVC, the frequency is determined as a ratio of the number of SVCs identified in a given SAGE II 1-km layer to the sample size at the layer of interest.

[9] In the following cloud anomaly analysis, the 1997/1998 El Niño measurements are compared with the 1985–1991 climatology as in the study of *Cess et al.* [2001b]. To enhance the presentation of the geographic dependence of the El Niño impact, the zonally averaged cloud occurrence frequency at a given latitude for a given altitude is removed from the 1997/1998 El Niño and climatological data sets in the analysis of longitude-latitude and longitude-altitude cloud anomaly distributions. Note, the difference in the data time frame between the 1997/1998 El Niño and the climatology is about 10 years. *Wang et al.* [2002] demonstrated the occurrence of decadal-scale changes in cloud frequency and OLR in the Tropics between 1985 and 1998 [see also *Wielicki et al.*, 2002]. Thus, the decadal changes in cloud occurrence would influence the El Niño anomaly analysis if they are not removed. To separate the decadal component and the El Niño changes completely is not straightforward. It is noted that the atmospheric response to El Niño sea surface temperature (SST) changes over the eastern Pacific is expected to be highly longitudinally dependent, while the decadal component of variation is

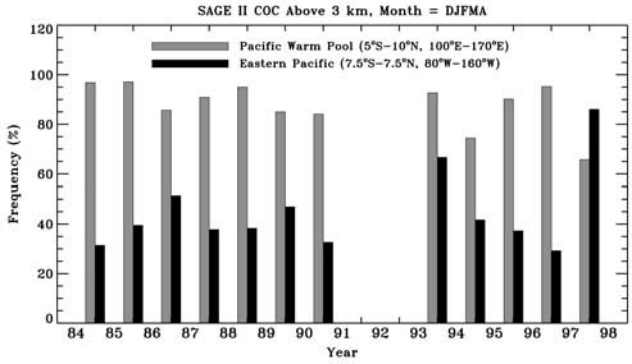

Figure 1. Time series record of the cumulative opaque cloud for the 5 months between December and April (DJFMA) over the Pacific warm pool and the eastern Pacific.

likely to be manifest in larger-scale features. Thus, it is possible to remove the decadal component of changes from the data analysis, to a large extent, by subtracting the corresponding zonally averaged cloud occurrence frequency (at a given altitude and a given latitude) from the respective SAGE II data sets.

[10] The SAGE II cloud count is equivalent to a binomial experiment with the cloud frequency as the binomial parameter [*Wang et al.*, 2001]. The associated uncertainty of the derived frequency is estimated by using the method of *Mendenhall and Scheaffer* [1973]. Geographic areas with an anomaly greater than the associated standard error estimation according to *Johnson and Bhattacharyya* [1992] are indicated by using a color graphic scheme in the present investigation.

2.1. Equatorial Cloud Distribution

[11] The study of *Cess et al.* [2001b] showed that, during the 1997/1998 El Niño, significant reductions in high-

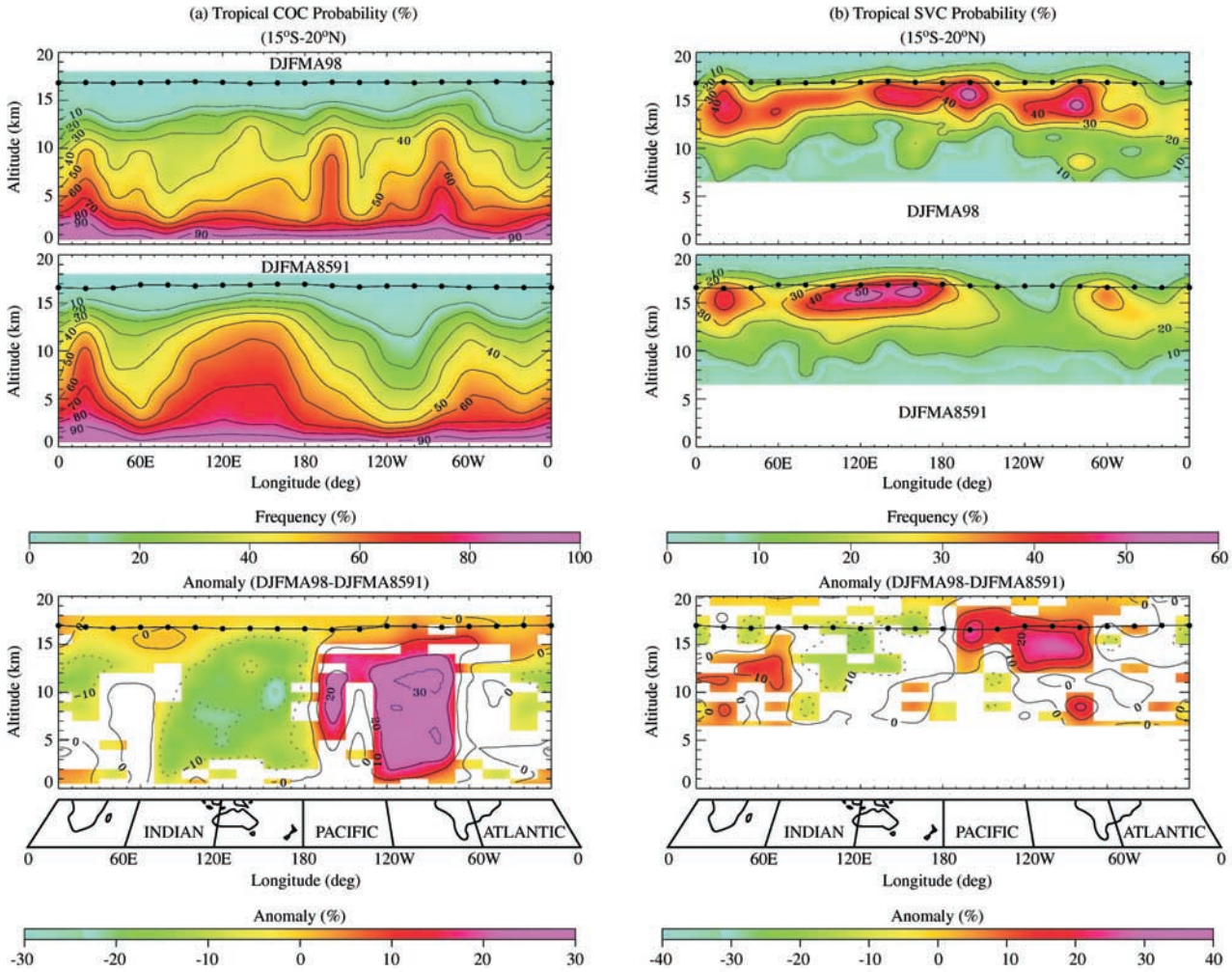

Figure 2. (a) (top) Tropical (15°S–20°N) cumulative opaque cloud distribution for the 1997/1998 El Niño, (middle) the 7-year DJFMA climatology, and (bottom) the cumulative opaque cloud anomalies. (b) (top) Tropical (15°S–20°N) subvisual cloud distribution for the 1997/1998 El Niño, (middle) the 7-year DJFMA climatology, and (bottom) the subvisual cloud anomalies. In the bottom panels, the colored regions indicate anomalies with values greater than the standard error. The line with black dots indicates the tropopause. The contour interval is 10% for both cloud occurrence frequency and for the anomaly.

altitude cloud occurrence over the Pacific warm pool (PWP) were coincident with dramatic enhancements of high-altitude clouds over the eastern Pacific (EP). To aid in the understanding of the impact of the 1997/1998 El Niño on the tropical cloud behavior, we present the time record of the COC above 3 km over the PWP and EP in Figure 1. The time series were constructed by computing the frequency of COC above 3 km for December through April (DJFMA) between 1985 and 1998. These 5 months correspond roughly to the second half of the mature period of the 1997/1998 El Niño. Because of the heavy aerosol loading from the June 1991 Pinatubo (15.1°N, 120.4°E) volcanic eruption, no SAGE II data are available in the troposphere in 1992 and 1993. The time record indicates that the COC over the PWP is more frequent than that over the EP throughout the data period with only one exception, 1998, indicating that the 1997/1998 event is unique.

[12] Figure 2a shows the COC height-longitude distribution across the entire tropics for the 1997/98 El Niño (DJFMA98) and the 7-year (1985–1991) DJFMA climatology (DJFMA8591), along with the anomalies. The tropical cloud distribution analysis is accomplished by using a data resolution of 20° (latitude) by 1 km (altitude). The El Niño COC distribution is quite different from the climatology. The normal broad areas of high clouds over the PWP and South America are supplanted during the El Niño by two distinct high-cloud towers. In addition, the COC frequency between 0°E and 180°E during the El Niño is much less than that of the climatology, particularly over the PWP. In the rest of the tropical regions, the results exhibit enhanced cloud over the west coast of South America and near 160°W. Particularly noteworthy is that most of the COC changes occurred at altitudes above 6 km, especially over the PWP, EP, and Africa. The analyses for SVC are shown in Figure 2b. Generally, the occurrence of SVC near the tropopause changed during the El Niño in a manner consistent with the tropical tropopause COC anomalies (Figure 2a). This eastward shift of the tropical SVC occurrence is also revealed in the measurement from the Halogen Occultation Experiment [*Massie et al.*, 2000].

[13] The pattern of the COC climatology in Figure 2a, characterized by a broad ridge of the COC centered over Indonesia and by a trough of the COC centered near 110°W, is exactly the type of cloud distribution expected to result from the Walker circulation, which features an upwelling branch over Indonesia and a subsiding branch over the eastern Pacific [see also *Wang et al.*, 1995b, 1998b]. Note that the COC climatology also reveals two additional ridges, over western South America and Africa, and two additional troughs, over the western Indian Ocean and the western Atlantic Ocean. Those equatorial ridges are known for regions of frequent deep convective activity. In contrast, during the El Niño, the tropical COC distributions reveal three ridges centered near the central Pacific, eastern Pacific, and Africa, reflecting a drastically different circulation pattern from the normal Walker cell [*Bell et al.*, 1999; *Cess et al.*, 2001b].

[14] To allow further understanding of the altered equatorial circulation, the El Niño temperature and pressure height anomalies in the Tropics calculated from the National Center for Environment Prediction (NCEP) reanalyses [*Kistler et al.*, 2001] are presented in Figures 3a and 3b,

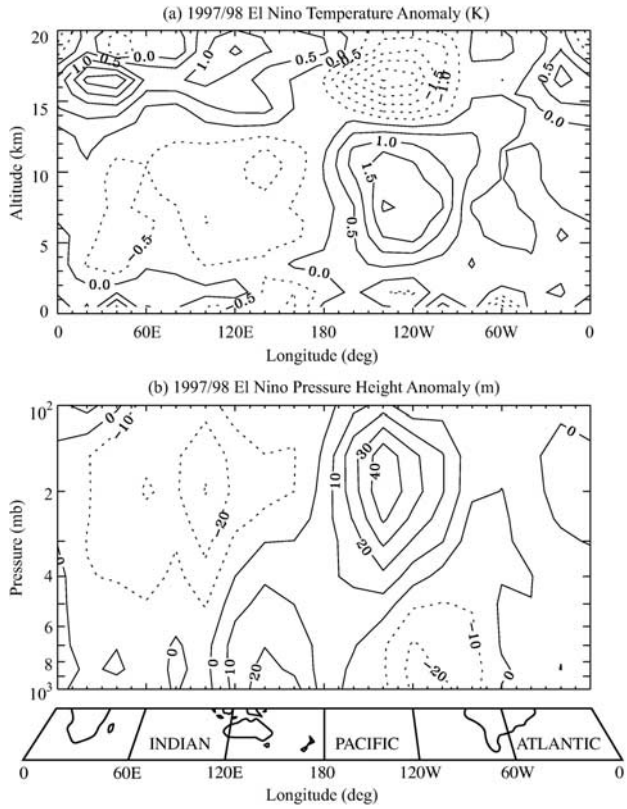

Figure 3. Anomalies of (a) temperature (contours, interval is 0.5 K), and (b) pressure-height (contour, interval is 10 m) in the tropics (15°S–20°N).

respectively. The outstanding features in Figure 3 include the distinct distributions of a region of negative temperature anomalies above a region of positive anomalies over the west of the date line. They are separated at an altitude of about 12 km. East of the date line, the vertical distribution of temperature anomalies, positive above and negative below 12 km, is opposite those west of the date line, although the magnitudes are somewhat smaller than those to the west. The associated pressure-height anomaly distribution in the lower troposphere below about 500 to 400 hPa shows negative pressure-height anomalies over the eastern Pacific and positive anomalies over Indonesia. In the upper troposphere, the pressure-height anomalies reverse sign with positive anomalies over the eastern Pacific and negative anomalies over Indonesia. These distributions are subject to the usual caveats associated with model analyses like the NCEP reanalyses [*Kalnay et al.*, 1996]. Uncertainties in a given parameter are likely to be larger in the oceanic tropics where surface observations are scarce.

[15] The distribution of the pressure-height anomaly in Figure 3 is consistent with that of the temperature anomaly through the hydrostatic relationship. Note, the vertical distribution of the pressure-height anomaly changes sign at a lower altitude than that of the temperature anomaly. This is because the pressure anomaly at a given altitude reflects the vertically integrated air density changes above that altitude. As a result, the level of zero pressure anomaly is located at an altitude above which the total of negative density changes is balanced by the total of positive density

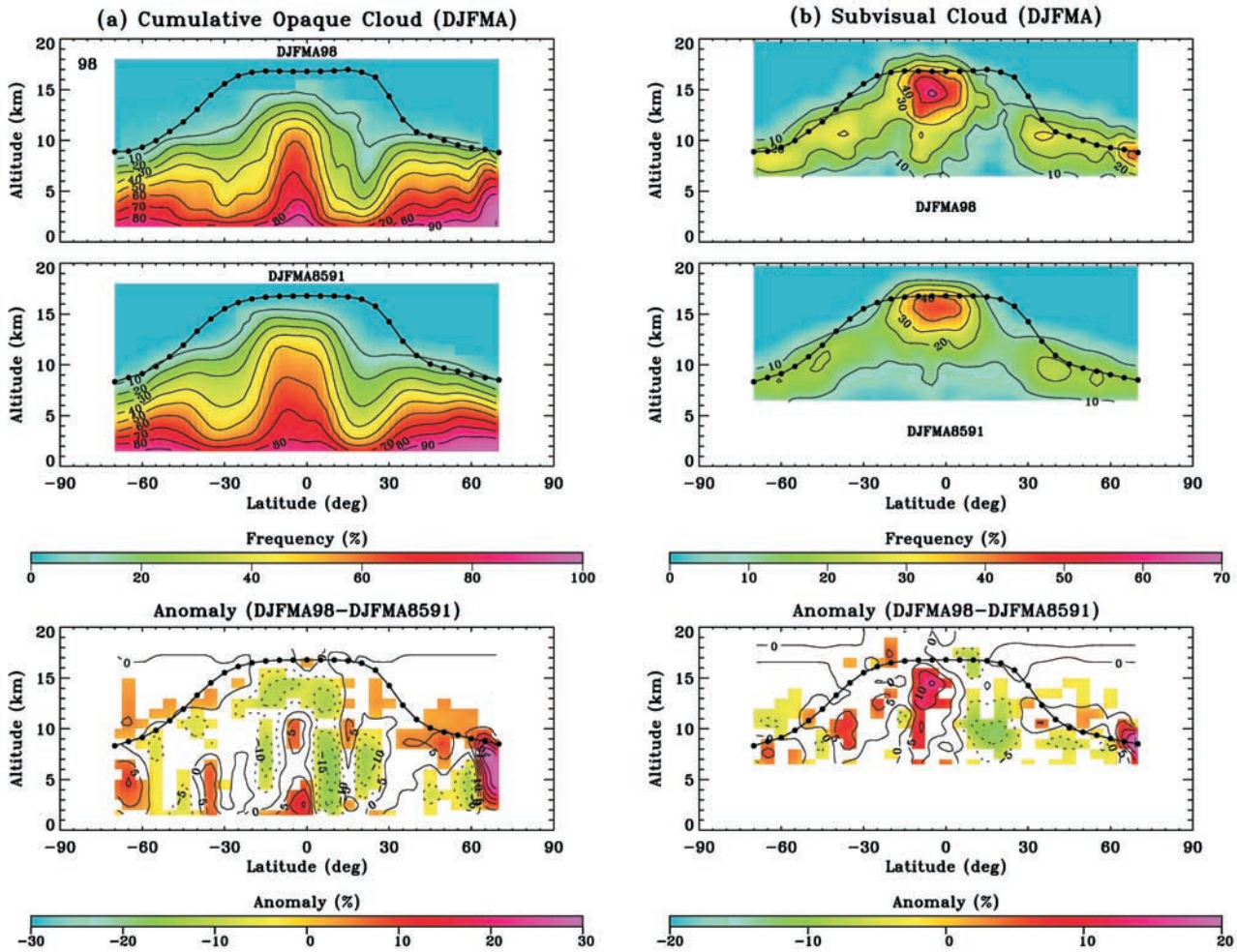

Figure 4. (a) (top) Zonal mean cumulative opaque cloud distribution for the 1997/1998 El Niño, (middle) the DJFMA climatology, and (bottom) the cumulative opaque cloud anomalies. (b) (top) Zonal mean subvisual cloud distribution for the 1997/1998 El Niño, (middle) the DJFMA climatology, and (bottom) the subvisual cloud anomalies. In the bottom panels, the colored regions indicate anomalies with values greater than the standard error. The line with black dots indicates the tropopause. The contour interval is 10% for cloud occurrence frequency and is 5% for the anomaly.

changes. The relationship between temperature, pressure, and density is governed by the ideal gas law, which is nonlinear. Generally, the negative temperature anomaly would induce negative density anomaly, leading to a situation in which the vertical distribution of the pressure anomaly changes sign at a lower altitude than that of the temperature anomaly. This pattern of pressure-height anomalies shown in Figure 3 would induce a component of reversed Walker circulation, leading to the observed cloud occurrence anomalies (Figure 2a) during the 1997/1998 El Niño. *Bell et al.* [1999] and *Cess et al.* [2001b] provide additional information on the altered Walker circulation.

2.2. Zonal Mean Features

2.2.1. COC and SVC

[16] The zonal mean COC for the 1997/98 El Niño and the 7-year climatology are presented in Figure 4a along with the anomalies. The cloud analysis includes 29 latitudinal bins with a bin width of 5° between 72.5°S and 72.5°N, as given by *Wang et al.* [1998b]. The COC patterns for both the climatology and the El Niño are typical with large frequencies in the tropics and extratropics and small frequencies in the subtropics. In the tropics, the distribution of tropical COC occurrence during the El Niño appears to be narrower and farther away from the tropopause than the climatology distribution. As seen in the anomaly analysis in Figure 4a, the COC frequency during the 1997/1998 El Niño is reduced in the northern Tropics and subtropics, except near 15°N. A large COC increase between 60°N and 70°N is also noticeable. At northern midlatitudes, the COC shows small increases near the tropopause and small decreases below about 6 km, especially near 60°N. In the Southern Hemisphere, the COC appears diminished, except in the southern tropics and the zones centered at about 35°S and 65°S. Overall, the mean COC in the tropics is decreased, particularly at altitudes above 11 km and around 6 km, consistent with the increased OLR and decreased reflected shortwave radiation determined from the ERBE nonscanner during the El Niño [*Wielicki et al.*, 2002]. The narrower and lower distribution of the zonal mean tropical

COC during the 1997/1998 El Niño relative to that of the climatology is very interesting. Because the area of subsidence associated with tropical deep convections is greater than that of ascending motion, the greatly intensified convective activities over the EP during the El Niño could be the reason for the apparent downward shift of the zonally averaged COC at high altitudes in tropics [see also *Wang et al.*, 2002].

[17] The corresponding zonal mean SVC analysis is presented in Figure 4b. The SVC increased over the tropics, with the center slightly shifted toward the Southern Hemisphere, and diminished over the northern subtropics and increased near the tropopause at northern high latitudes. In the Southern Hemisphere, the SVC exhibits enhancements equatorward of 45°S in the upper troposphere. Small SVC reductions are also evident just above the tropopause at southern high latitudes.

2.2.2. Tropospheric Meridional Circulation

[18] As cloud vertical variations can serve as a proxy of convective activities, *Wang et al.* [1998b] developed a simple and robust model for diagnosis of the tropospheric mean meridional circulation based on zonal mean opaque cloud distributions derived from the SAGE II observations. Briefly, the model assumes that, at a given altitude, the local zonal mean vertical velocity w (z, θ) is a linear function of the local departure of the COC occurrence frequency, Δf (z, θ), from the corresponding global mean, i.e.,

$$w(z,\theta) = \kappa \Delta f(z,\theta) \tag{1}$$

where z is the altitude, θ indicates the latitude, and κ is a proportional constant. As we can see, the proportional constant κ relates the vertical velocity distribution to the cloud field. In practice, the coefficient κ serves as a calibration coefficient in an experimental sense. A value of 8.3×10^{-5} m/s [*Wang et al.*, 1998b] was determined based on a combination of the vertical circulation climatologies of *Schubert et al.* [1990], *Peixoto and Oort* [1992], and *Trenberth* [1992]. The continuity equation is then used to infer the meridional velocity field from the vertical circulation. The seasonal variations of the derived model circulation have been shown to be very consistent with the SAGE II tropospheric ozone and aerosol 1.02-μm measurements. The readers are referred to *Wang et al.* [1998b] for a more detailed presentation of the mean meridional circulation model.

[19] The derived mean meridional circulation for both the 1997/98 El Niño and the corresponding climatology are presented in Figure 5. Shown also in Figure 5 is the distribution of the mean circulation difference (vector wind anomaly) between the El Niño and the climatology, keeping in mind that the mean circulation difference involves changes in flow direction as well as flow speed. The circulation pattern during the 1997/1998 El Niño differs from that of the climatology in many respects. In the Tropics, the ascending branch of the Hadley cell during the El Niño is narrower and stronger than that of the climatology. A derived mean vertical velocity of 32×10^{-4} m/s during the peak of the El Niño is located at an altitude of 9 km near 5°S, which is about a 20% increase over that of the normal year. In the Northern Hemisphere (NH), the indirect circulation cell during the El Niño is intensified with a much wider latitudinal extension than that of the climatology. It stretches from the subtropical region to high latitudes, and appears to push the polar direct thermal cell closer to the pole. In addition, during the 1997/1998 El Niño, the northern Hadley cell appears to expand further to the north near the tropopause and shows less vertical extension of the tropical ascending branch than that of the climatology. Comparatively, the Hadley cell in the Southern Hemisphere (SH) during the El Niño appears to be diminished slightly, except the poleward branch of the circulation. A poleward stretch of the SH indirect circulation cell is also noticeable. Overall, the mean circulation difference distribution is consistent with the latitude-altitude distribution of COC anomalies shown in Figure 4a, as expected.

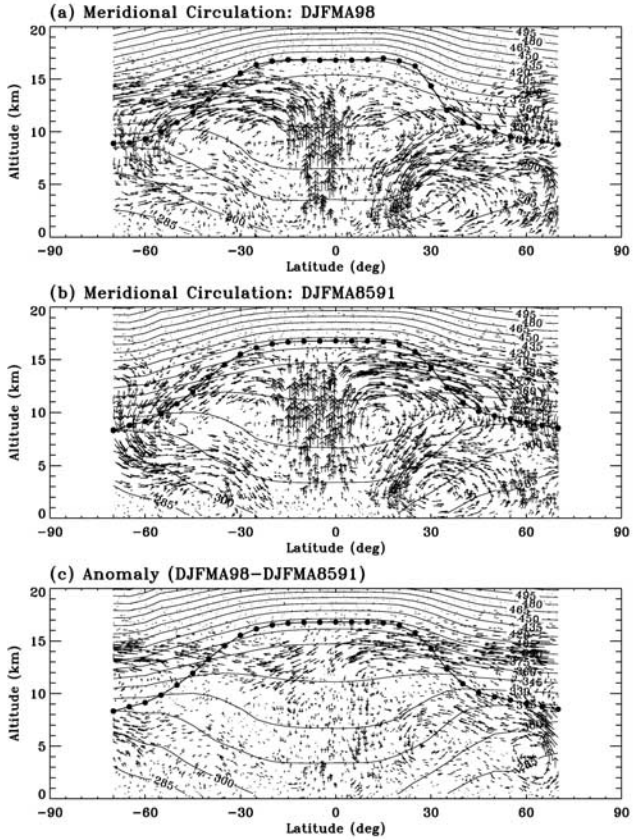

Figure 5. Tropospheric mean meridional circulation for (a) the 1997/1998 El Niño, and (b) the DJFMA climatology. (c) Mean circulation difference (DJFMA98 - DJFMA8591). The line with black dots represents the tropopause. The solid lines indicate constant potential temperature with a contour interval of 15 K.

[20] It should be noted that the midlatitude troposphere experienced a series of pronounced anomalies on a monthly to seasonal time scale during the 1997/1998 El Niño period [*Bell et al.*, 1999]. Furthermore, the response of the atmosphere to the 1997/1998 El Niño is hemispherically asymmetric, as discussed by *Peng and Van den Dool* [1998], who showed that the tropical forcing plays a major role in generating the midlatitude circulation anomalies mainly during winter months. Note, the feature in Figure 5 represents the zonally averaged circulation system. Because the atmospheric response to the El Niño sea surface temperature

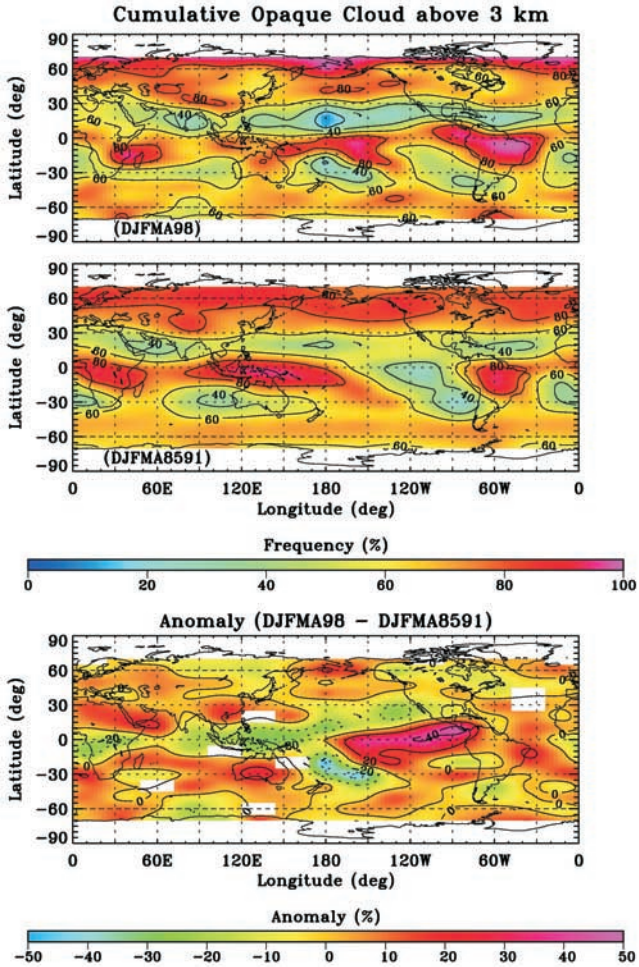

Figure 6. Latitude-longitude distribution of cumulative opaque cloud above 3 km for the 1997/98 El Niño (upper panel), the DJFMA climatology (middle panel), and the anomalies (bottom panel). In the bottom panel, the colored regions indicate anomalies with values greater than the standard error. The contour interval is 20% for both the cloud occurrence frequency and the anomaly.

changes is highly longitudinally dependent, caution must be exercised when interpreting the results presented in Figure 5. It should also be stated that, although the simple model inferred mean meridional circulation from the zonally averaged COC distribution is very interesting and useful, the model results are unlikely to simulate perfectly the real circulation.

2.3. Cloud Longitude-Latitude Distributions

[21] The cloud distribution was derived for 10°-latitude by 24° -longitude grids as in the 6-year cloud climatology of *Wang et al.* [1996]. Because of the solar occultation technique and the ERBS orbital characteristics, the number of overpasses of the SAGE II instrument is lower in the Tropics than elsewhere [*McCormick*, 1987]. This fact, together with the frequent opaque cloud presence, substantially limits the number of observations at tropical lower altitudes. On average, during the 5 months (DJFMA) at the peak of the El Niño, the total number of overpasses is about 35, while only about 13 samples are taken for the 10° × 24° grids at 3 km [*Wang et al.*, 2001]. For the above reasons, we present the COC distributions above 3 km. Because the climatology is a multiyear (1985–1991) data ensemble, the number of samples is about 7 times larger than during the El Niño.

2.3.1. COC

[22] The distributions of the COC above 3 km for the El Niño are displayed in Figure 6, together with the 7-year COC climatology and the El Niño anomalies. The areas in the Northern Hemisphere with the climatological COC minima (COC < 40%) were intensified during the El Niño, while the minima regions in the Southern Hemisphere either became less pronounced or shifted longitudinally. The tropical maxima areas (COC > 80%) shifted longitudinally and shrank, except over South America and the EP. Movement of the minima region in the South Pacific to the east of Australia resulted in the large negative anomaly in the South Pacific (<−30%) and the large positive anomaly over Australia. The huge positive anomaly over the EP and the outstanding wishbone shape of the negative anomalies around the equator resemble the pattern of the National Oceanic and Atmospheric Administration (NOAA) Reynolds SST anomalies seen in Figure 7, as well as the precipitation anomalies over the Pacific obtained by merging rain gauge observations and satellite-derived precipitation estimates [*Bell et al.*, 1999].

[23] Northeastern Brazil and the Amazon Basin are typically drier during the winter/spring of El Niño events [*Hastenrath*, 1991] [see also *Bell et al.*, 1999, Figure 22]. Thus, the cloud anomaly over Northeast Brazil and the Amazon Basin shown in Figure 6, appears to be inconsistent with the precipitation observations [*Bell et al.*, 1999, Figure 22] and the earlier record of *Hastenrath* [1991]. The reason for the South American inconsistency is not obvious. Part of the inconsistency may result from differences in the selected background climatologies. The present results are referenced to the SAGE II cloud observations for December through April, 1985–1991, while the precipitation measurements between 1979 and 1995 were used by *Bell et al.* [1999] as the baseline climatology. Some differences are also expected because the SAGE II instrument detects many high-altitude thin cirrus clouds with vertical optical depth between 0.03 and 0.3, particularly in the tropics [*Wang et al.*, 1996, 1998b]; for example, the outflow of large-scale high-altitude anvil cirrus from tropical deep convective

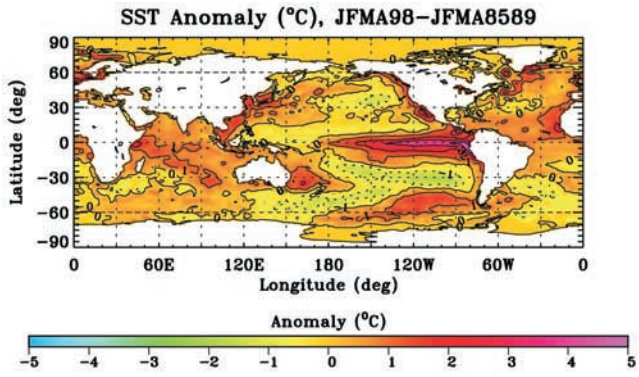

Figure 7. Latitude-longitude distribution of the sea surface temperature (SST) anomaly (JFMA98-JFMA8589). The temperature anomaly contour interval is 1°C.

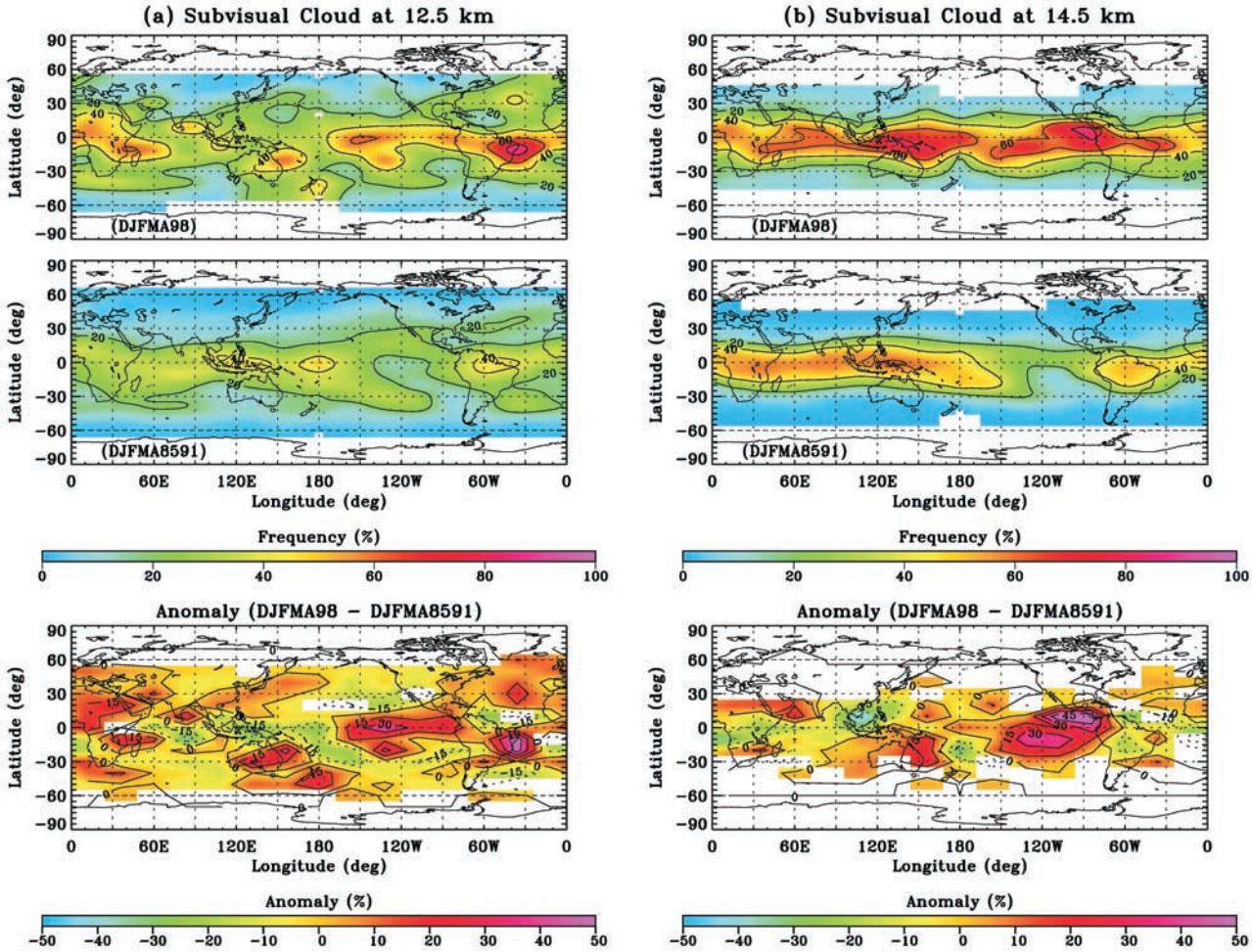

Figure 8. (a) (top) Latitude-longitude distributions of subvisual cloud at 2.5 km for the 1997/1998 El Niño, (middle) the DJFMA climatology, and (bottom) the anomalies. (b) The same as in Figure 8a but for subvisual cloud at 14.5 km. In the bottom panels, the colored regions indicate anomalies with values greater than the standard error. The contour interval is 20% for cloud occurrence frequency and is 15% for the anomaly.

systems. These thin cirrus clouds have a small impact on the OLR and are not necessarily related to precipitation. The South American inconsistency is further explored below.

[24] Despite the drastic changes in horizontal and vertical distributions of cloud occurrence, the estimated mean COC occurrence above the 3-km level for 70°S to 70°N during the El Niño is about 47%, which is only 2% less than the corresponding climatological mean. This feature appears to imply that the global coverage of upward motion associated with the large-scale circulation is roughly the same as that of the downward motion.

2.3.2. SVC

[25] The SVC distribution at 12.5 km during the 1997/98 El Niño is displayed in Figure 8a, along with the corresponding climatology and the SVC anomalies. The SVC coverage is enhanced over the eastern central Pacific, tropical eastern South America, and central Africa, and is reduced over the western Pacific and Indonesia. Generally, the SVC occurrence exhibits an anomaly pattern similar to the COC results (Figure 6). The analysis of the SVC at 14.5 km is presented in Figure 8b. The distribution of SVC anomalies at 14.5 km is somewhat different from that at 12.5 km. The main features are the great enhancement of SVC over the eastern Pacific and eastern Australia and adjacent Pacific Ocean, and reduced SVC over the South China Sea and northern Indonesia.

3. Cloud Longwave Radiative Forcing

[26] Clouds play crucial roles in the Earth radiation budget. They interact with both solar and terrestrial radiation [e.g., *Liou*, 1992]. As a further illustration of the impact of the 1997/1998 El Niño on the Earth-atmosphere system, the cloud observations from SAGE II have been used to estimate changes in cloud longwave radiative forcing, and the results are compared with the ERBE/CERES scanner CLRF anomaly measurements. This estimation employs the cloud longwave radiative forcing model of *Ramanathan* [1977],

$$F = C \times \epsilon \times A \times (T_c - T_g) \tag{2}$$

where F is CLRF, C is a model coefficient, ϵ the cloud effective emissivity, A the cloud frequency, T_c the cloud

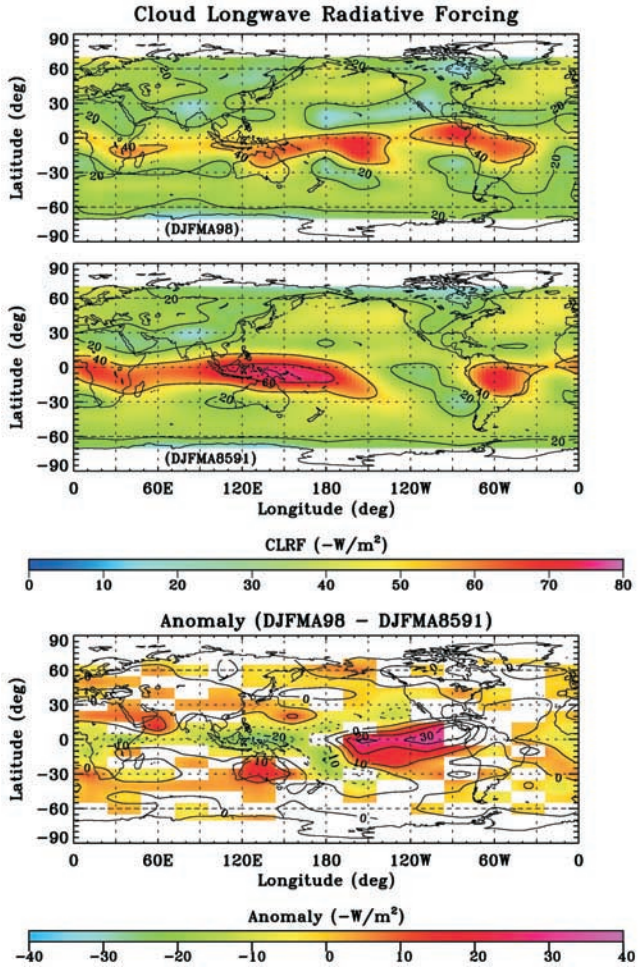

Figure 9. (top) Latitude-longitude distribution of SAGE II model calculation of the cloud longwave radiative forcing for the 1997/1998 El Niño, (middle) the DJFMA climatology, and (bottom) the anomalies. In the bottom panel, the colored regions indicate anomalies with values greater than the standard error. The contour interval is 20 W/m^2 for cloud longwave radiative forcing and is 10 W/m^2 for the anomaly.

temperature, and T_g the surface temperature. *Ramanathan* [1977] suggests a value of 1.65 W/m^2/K for C. A recent study by *Wang et al.* [2002], based on cloud radiative transfer studies of *Fu and Liou* [1992, 1993] and *Kiehl* [1993], yields C = 2.24 W/m^2/K, the value used here. *Wang et al.* [2002] determined a mean of 0.36(±0.003) for ϵ and a linear trend in ϵ of −0.026(±0.008)/decade for the tropics during 1985–1998. Accordingly, the mean effective emissivities of 0.37 and 0.34 are used for the 7-year climatology and the 1997/1998 El Niño, respectively, in the present investigation. As in the study of *Wang et al.* [2002], we use the occurrence frequency of the uppermost opaque cloud (UOC) [*Wang et al.*, 2001] for the CLRF study, because the CLRF depends primarily on the physical properties (emissivity and temperature) of the uppermost cloud systems.

[27] According to *Wang et al.* [1998c], the mean optical depth for SAGE II SVC is about 3.5 × 10^{-2} at a 1.02-μm wavelength. Assuming that the SVC particles are ice spheres with a mean effective radius of 1 μm and an effective variance of 1, Mie scattering calculations yield an extinction efficiency 2.28 at 1.02 μm, and an extinction efficiency of 0.355 at 10.8 μm [*Wang et al.*, 1996]. Thus, the mean visible optical depth of 3.5 × 10^{-2} converts to an optical depth of 5 × 10^{-3} for longwave (10.8 μm). For cloud with very small optical depth, the emissivity is roughly equal to the value of the optical depth. Thus, the emissivity of the SAGE II SVC is about 5 × 10^{-3}. For the SAGE II UOC, the emissivity is estimated to be 0.36 [*Wang et al.*, 2002]. This value is close to the cirrus cloud emissivity of 0.35 of *Paltridge and Platt* [1976, Table 8.1]. As mentioned in section 2, the SAGE II opaque clouds generally include all types of clouds, except SVCs. Therefore, approximately, the emissivity of SVC is about 2 orders of magnitude smaller than that of UOC. For this reason, only the UOC frequencies are included in the CLRF analysis. The meteorological data, including surface temperature and tropospheric temperature from the NCEP reanalyses, are incorporated in the CLRF investigation. The model CLRF calculation is performed for each of the SAGE II layers for each geographic bin. Vertical integration of the derived F is then carried out to determine the total CLRF.

[28] The model-calculated CLRF results for the 1997/1998 El Niño and the corresponding climatology, together with the anomalies, are shown in Figure 9. Outstanding features of the CLRF climatology are the large magnitude of CLRF (about −40 W/m^2) over the PWP, Indonesia, northern South America, and tropical Africa. (The negative sign means reduced outgoing longwave radiation resulting from cloud presence.) During the 1997/1998 El Niño, the magnitude of the CLRF over those regions is significantly reduced, implying increased OLR. Concurrent with those changes is the greatly enhanced CLRF over the EP, corresponding to significantly reduced OLR. The distributions of the model-calculated CLRF anomalies during the 1997/1998 El Niño are generally consistent with those derived from the ERBE/CERES scanner observations shown in Figure 10, although the magnitude is slightly smaller over the tropical central Pacific. The large white areas in Figure 9

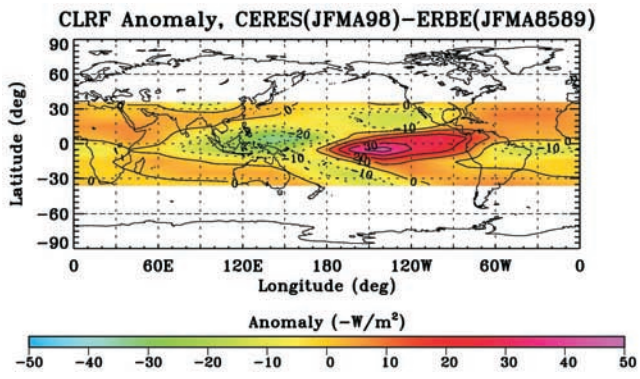

Figure 10. Latitude-longitude distribution of outgoing longwave radiation (OLR) anomaly derived from the ERBE/CERES scanner observations. The ERBE observations consist of measurements obtained in the 4 months January–April from 1985 to 1989, and the CERES data are collected during the 4 months in 1998. The OLR anomaly contour interval is 10 W/m^2.

represent the locations where the derived CLRF is statistically insignificant. The combination of the SAGE II sampling and the use of a single value for ϵ for the tropics [*Wang et al.*, 2002] as well as the natural variability of the OLR diminish the reliability of the estimates in these areas. Elsewhere, the SAGE-II estimates of CLRF are within about +10 W/m^2 of the ERBE/CERES results (Figure 10). The apparent increase in COC over northeastern Brazil during the El Niño in Figure 6 may be accompanied by a decrease in ϵ resulting in cancellation of effects in the OLR. The OLR anomalies over northeastern Brazil reported by *Bell et al.* [1999] are very small as suggested by the anomaly results in both Figures 9 and 10. Thus, the decrease in precipitation over northeastern Brazil that typically accompanies an El Niño does not necessarily dictate a blanket decrease in cloud cover. Figures 9 and 10 demonstrate that the SAGE II analysis can isolate the locations and magnitudes of the largest OLR anomalies. To the authors' knowledge, the present study is the first of its kind to provide a direct, quantitative link between satellite measurements of cloud frequency and CLRF obtained during the unique 1997/1998 El Niño. These results should aid the understanding of the cloud-radiation interactions that occurred during the event.

4. Conclusions and Remarks

[29] This study has examined the characteristics of cloud distributions and mean tropospheric circulations during the 1997/1998 El Niño, based on the observations from the SAGE II satellite instrument. These observations provide a unique three-dimensional characterization of the mean cloud frequency distribution over much of the globe. In addition, the SAGE II model-calculated cloud longwave radiative forcing associated with this unusual El Niño has been analyzed and related to that derived from the ERBE/CERES observations.

[30] The results reveal that, during the 1997/1998 El Niño, (1) the high-altitude opaque cloud occurrence frequency increased dramatically over the eastern tropical Pacific and decreased at almost the same magnitude over the Pacific warm pool, generally consistent with the pattern of the tropical sea surface temperature and precipitation anomalies; (2) the subvisible cloud frequency variations generally are similar to those of the opaque clouds near the tropopause; (3) the anomalies of the zonally averaged cloud distributions are characterized by reduced OCs at low latitudes, except in the southern tropics below 10 km, and enhanced OCs at high latitudes, along with increased SVCs in the southern tropics and decreased SVCs in the northern subtropics in the upper troposphere; (4) the model-calculated CLRF anomalies based on SAGE II cloud data yield a geographic distribution that is consistent generally with the CLRF anomalies derived from the ERBE/CERES measurements; (5) the cloud height-longitude distribution in the tropics reflects a severely perturbed Walker circulation over the Pacific Ocean; and (6) the tropospheric mean meridional circulation is characterized by an intensified indirect thermal circulation cell that appears to be stretched poleward in the Northern Hemisphere, and a slightly weakened circulation system in the Southern Hemisphere, except the poleward branch of the Hadley circulation.

[31] The uniqueness of the cloud structure during the 1997/1998 El Niño largely reflects the unusual circulation system associated with the distinct El Niño. The unusual circulation pattern is primarily the atmospheric response to the evolution of the sea surface temperature distribution over the tropical eastern Pacific during this strong 1997/1998 El Niño. The sudden switch of circulation patterns and the associated cloud distributions, so different from previous El Niños, is likely due to the greater rate of change and enhancement of SST over the tropical eastern Pacific during early 1997 than during typical El Niños. This initial period is then followed by a long period of high SSTs (near 29°C) from May 1997 through early May 1998 [*Kousky*, 1998; *Bell et al.*, 1999]. As indicated by *Cess et al.* [2001a], the SST distribution averaged from January to August 1998 over the tropical Pacific is longitudinally more uniform, with an SST difference of 2°C in the zonal direction across the entire tropical Pacific and the Indian Ocean, in contrast to the 4°C difference for a normal year. The nearly uniform SST over the tropical Pacific, during the peak of the 1997/1998 El Niño, results in drastically intensified convective activity over the tropical eastern Pacific, leading to collapse of the Walker circulation [*Kousky*, 1998; *Cess et al.*, 2001b], and strengthened Hadley circulation over the eastern Pacific [*Wong et al.*, 2000; *Cess et al.*, 2001b].

[32] As indicated in section 2, the component of zonally averaged cloud frequency was removed from the anomaly analyses of the longitudinal dependence of the cloud frequency to avoid contamination from the decadal component of cloud changes. This is because the focus of the present study is on the cloud anomaly associated with the 1997/1998 El Niño. *Wang et al.* [2002] have studied the decadal cloud changes in the Tropics recently. The decadal changes in zonally averaged cloud occurrence frequency in the extratropics will be investigated in detail separately.

[33] The general consistency between the SAGE II model calculated CLRF and the CLRF anomaly derived from the ERBE/CERES observations during the 1997/1998 El Niño presented here provides additional evidence of the intimate connection between clouds and OLR, and further strengthens the confidence in long-term cloud and OLR measurements from remote sensing satellite systems that are crucial to the detection and understanding of climate changes [*Asrar et al.*, 2001]. Moreover, as clouds constitute the primary source of uncertainties in existing general circulation and climate models as a result of poor cloud parameterization schemes [*Intergovernmental Panel on Climate Change*, 2001], the observed cloud structure changes from the SAGE II instrument during this unique 1997/1998 El Niño and the resulting impact of the El Niño on outgoing longwave radiation detected by ERBE/CERES, should be highly valuable for validating and improving cloud-radiation-climate interactions in general circulation and climate models.

[34] **Acknowledgments.** The authors would like to thank W. P. Chu and C. R. Trepte of the NASA Langley Research Center for helpful comments and discussions on the investigation. We also want to thank three anonymous reviewers for constructive comments and suggestions on an earlier version of the manuscript. P.-H. Wang and G. S. Kent are supported by the NASA OES SAGE Project through contracts NAS1-99129, NAS1-02058, and NAS1-18941.

References

Asrar, G., J. A. Kaye, and P. Morel, NASA research strategy for Earth system science: Climate component, *Bull. Am. Meteorol. Soc.*, *82*, 1309–1329, 2001.

Barkstrom, B. R., The Earth Radiation Budget Experiment (ERBE), *Bull. Am. Meteorol. Soc.*, *65*, 1170–1185, 1984.

Bell, G. D., M. S. Halpert, C. F. Ropelewski, V. E. Kousky, A. V. Douglas, R. C. Schnell, and M. E. Gelman, Climate assessment for 1998, *Bull. Am. Meteorol. Soc.*, *80*, S1–S48, 1999.

Bregman, B., P.-H. Wang, and J. Lelieveld, Chemical ozone loss in the tropopause region on subvisible ice clouds, calculated with a chemistry-transport model, *J. Geophys. Res.*, *107*(D3), 4032, 10.1029/2001JD000761, 2002.

Cess, R. D., M. Zhang, B. Wielicki, D. F. Young, X.-L. Zhou, and Y. Nikitenko, The influence of the 1998 El Niño upon cloud-radiative forcing over the Pacific warm pool, *J. Clim.*, *14*, 2129–2137, 2001a.

Cess, R. D., M. Zhang, P.-H. Wang, and B. Wielicki, Cloud structure anomalies over the tropical Pacific During the 1997/98 El Niño, *Geophys. Res. Lett.*, *28*, 4547–4550, 2001b.

Fu, Q., and K.-N. Liou, On the correlated k-distribution method for radiative transfer in nonhomogenous atmospheres, *J. Atmos. Sci.*, *49*, 2139–2156, 1992.

Fu, Q., and K.-N. Liou, Parameterization of the radiative properties of cirrus clouds, *J. Atmos. Sci.*, *50*, 2008–2025, 1993.

Hastenrath, S., *Climate Dynamics of the Tropics*, 488 pp., Kluwer Acad., Norwell, Mass., 1991.

Intergovernmental Panel on Climate Change, *Climate Change 2001: The Scientific Basis*, edited by J. T. Houghton et al., pp. 49–50, Cambridge Univ. Press, New York, 2001.

Johnson, R. A., and G. Bhattacharyya, *Statistics: Principles and Methods*, 682 pp., John Wiley, New York, 1992.

Kalnay, E., et al., The NCEP/NCAR 40-year reanalysis project, *Bull. Am. Meteorol. Soc.*, *77*, 437–471, 1996.

Kent, G. S., D. M. Winker, M. T. Osborn, M. P. McCormick, and K. M. Skeens, A model for the separation of cloud and aerosol in SAGE II occultation data, *J. Geophys. Res.*, *98*, 20,725–20,735, 1993.

Kiehl, J. T., On the observed near cancellation between longwave and shortwave cloud forcing in tropical regions, *J. Clim.*, *7*, 559–565, 1993.

Kistler, R., et al., The NCEP-NCAR 50-year reanalysis: Monthly means CD-ROM and documentation, *Bull. Am. Meteorol. Soc.*, *82*, 247–267, 2001.

Kousky, V., The 1997–98 Warm (El Niño) Episode: Onset and decay stages, Paper presented at 23rd Annual Climate Diagnostics and Prediction Workshop, U.S. Dep. of Commerce, Miami, Fla., 1998.

Liou, K. N., *Radiation and Cloud Processes in the Atmosphere*, pp. 487, Oxford Univ. Press, New York, 1992.

Massie, S., P. Lowe, X. Tie, M. Hervig, G. Thomas, and J. Russell III, Effect of the 1997 El Niño on the distribution of upper tropospheric cirrus, *J. Geophys. Res.*, *105*, 22,725–22,741, 1997.

McCormick, M. P., SAGE II: An overview, *Adv. Space Res.*, *7*, 319–326, 1987.

McCormick, M. P., P. Hamill, T. G. Pepin, W. P. Chu, T. J. Swissler, and L. R. McMaster, Satellite studies of the stratospheric aerosols, *Bull. Am. Meteorol. Soc.*, *60*, 1038–1049, 1979.

McPhaden, M. J., The 1997–98 El Niño, paper presented at 23rd Annual Climate Diagnostics and Prediction Workshop, U.S. Dep. of Commerce, Miami, Fla., 1998.

Mendenhall, W., and R. L. Scheaffer, *Mathematical Statistics with Applications*, 581 pp., Duxbury, Boston, Mass., 1973.

Paltridge, G. W., and C. M. R. Platt, *Radiative Processes in Meteorology and Climatology*, 318 pp., Elsevier Sci., New York, 1976.

Peixoto, J. P., and A. H. Oort, *Physics of Climate*, 520 pp., Am. Inst. of Phys., New York, 1992.

Peng, P., and H. Van den Dool, The impact of 1997/98 El Niño on the mid-latitude atmospheric circulation as evaluated by a steady state linear model, paper presented at 23rd Annual Climate Diagnostics and Prediction Workshop, U.S. Dep. of Commerce, Miami, Fla., 1998.

Ramanathan, V., Interactions between ice-albedo, lapse-rate and cloud top feedbacks: An analysis of the nonlinear response of a GCM climate model, *J. Atmos. Sci.*, *34*, 1885–1897, 1977.

Sassen, K., and B. S. Cho, Subvisual-thin cirrus lidar dataset for satellite verification and climatological research, *J. Appl. Meteorol.*, *31*, 1275–1285, 1992.

Schubert, S., C.-K. Park, W. Higgins, S. Moorthi, and M. Suarez, An atlas of ECMWF analyses (1980–1987), I, First moment quantities, *NASA Tech. Memo., 100747*, 1990.

Solomon, S., S. Borrmann, R. R. Garcia, R. Portmann, L. Thomason, L. R. Poole, D. Winker, and M. P. McCormick, Heterogeneous chlorine chemistry in the tropopause region, *J. Geophys. Res.*, *102*, 21,411–21,429, 1997.

SPARC, *Assessment of upper tropospheric and stratospheric water vapour*, *WMO/TD 1043, SPARC Rep. 2*, World Meteorol. Organ., Geneva, December, 2000.

Trenberth, K. E., Global analyses from ECMWF and atlas of 1000 to 10 mb circulation statistics, *NCAR TN-373+STR*, Natl. Cent. for Atmos. Res., Boulder, Colo., 1992.

Wang, C., P. J. Crutzen, V. Pamanathan, and S. F. Williams, The role of a deep convective storm over the tropical Pacific Ocean in the redistribution of atmospheric chemical species, *J. Geophys. Res.*, *100*, 11,509–11,516, 1995a.

Wang, P.-H., SAGE II tropospheric measurement frequency and its meteorological implication (reprint), paper presented at Seventh Conference on Satellite Meteorology and Oceanography, Am. Meteorol. Soc., Boston, Mass., 1994.

Wang, P.-H., et al., Tropical high cloud characteristics derived from SAGE II extinction measurements, *Atmos. Res.*, *34*, 53–83, 1994.

Wang, P.-H., M. P. McCormick, P. Minnis, G. S. Kent, G. K. Yue, and K. M. Skeens, A method for estimating vertical distribution of the SAGE II opaque cloud frequency, *Geophys. Res. Lett.*, *22*, 243–246, 1995b.

Wang, P.-H., P. Minnis, M. P. McCormick, G. S. Kent, and K. M. Skeens, A 6-year climatology of cloud occurrence frequency from SAGE II observations (1985–1991), *J. Geophys. Res.*, *101*, 29,407–29,429, 1996.

Wang, P.-H., G. S. Kent, G. K. Yue, K. A. Powell, L. R. Poole, and H. M. Steele, Simulation of SAGE II tropical particulate extinctions near the tropopause using a simple microphysical model, *OSA Tech. Dig., Cirrus*, 78–80, 1998a.

Wang, P.-H., D. Rind, C. R. Trepte, G. S. Kent, G. K. Yue, and K. M. Skeens, An empirical model study of the tropospheric meridional circulation based on SAGE II observations, *J. Geophys. Res.*, *103*, 13,801–13,818, 1998b.

Wang, P.-H., P. Minnis, M. P. McCormick, G. S. Kent, G. K. Yue, D. F. Young, and K. M. Skeens, A study of the vertical structure of tropical (20°S–20°N) optically thin clouds from SAGE II observations, *Atmos. Res.*, *47–48*, 599–614, 1998c.

Wang, P.-H., R. E. Veiga, L. B. Vann, P. Minnis, and G. S. Kent, A further study of the method for estimation of SAGE II opaque cloud occurrence, *J. Geophys. Res.*, *106*, 12,603–12,613, 2001.

Wang, P. H., P. Minnis, B. A. Wielicki, T. Wong, and L. B. Vann, Satellite observations of long-term changes in tropical cloud and outgoing longwave radiation from 1985 to 1998, *Geophys. Res. Lett.*, *29*, 1397, 10.1029/2001GL014264, 2002.

Wielicki, B. A., et al., Evidence for large decadal variability in the tropical mean radiative energy budget, *Science*, *295*, 841–844, 2002.

Wong, T., D. F. Young, M. Haeffelin, and S. Weckmann, Validation of the CERES/TRMM ERBE-like monthly mean clear-sky longwave dataset and the effects of the 1998 ENSO event, *J. Clim.*, *13*, 4256–4267, 2000.

R. D. Cess and M. Zhang, Marine Sciences Research Center, State University of New York, Stony Brook, Stony Brook, NY 11794-5000, USA. (rcess@notes.cc.sunysb.edu; mzhang@notes.cc.sunysb.edu)

G. S. Kent and P.-H. Wang, STC/NASA-LaRC, MS 475, Hampton, VA 23681-2199, USA. (g.s.kent@larc.nasa.gov; p.wang@larc.nasa.gov)

P. Minnis, B. A. Wielicki, and T. Wong, NASA-LaRC, MS 420, Hampton, VA 23681-2199, USA. (p.minnis@larc.nasa.gov; b.a.wielicki@larc.nasa.gov; takmeng.wong@larc.nasa.gov)

L. B. Vann, NASA-LaRC, MS 420, Hampton, VA 23681-2199, USA. (l.b.vann@larc.nasa.gov)